Jour. Petrol. Soc. Korea
Vol. 5, No. 1, p. 21~34, 1996

Fluid-rock Interaction during Contact Metamorphism of the Hwanggangni Formation Geosan, Korea

Sangmyung Kim and Hyung Shik Kim

Department of Earth and Environmental Sciences, Korea University, 5-1, Anam-dong, Sungbuk-ku, Seoul, 136-701, Korea

ABSTRACT : Contact-metamorphosed calc-silicate hornfels of the Hwanggangni formation adjacent to Daeyasan granite in Goesan are characterized by the mineral assemblages, tremolite-clinozoisite-alkali feldspar-calcite, diopside-grossular-vesuvianite, and wollastonite-diopside-phlogopite-grossular-vesuvianite, indicating low X_{co_2} condition during contact metamorphism. Two trends of fluid-rock interactions are recognized; combination of infiltration and buffering in the outer portion of the aureole and fluid-dominated behavior in the most part of the aureole. Modal abundance of diopside produced during metamorphism was measured in order to estimate fluid/rock ratios and permeabilities with the assumption that equivalent volume of fluids estimated from the fluid/rock ratios flow through the rock body. The calculated fluid/rock ratios and permeabilities range from 0.6 to 9 and 10^{-19} to 10^{-17} m^2, respectively. These values are in good agreement with previously calculated permeabilities in the calc-silicate hosted contact aureoles and expected values during progressive metamorphism by theories.

Key words : fluid-rock interaction, fluid-rock ratio, permeability, calc-silicate hornfels

INTRODUCTION

Fluids has long been recognized as an important agent during both contact and regional metamorphism, since they may control the stability and evolution of mineral assemblages, and heat transport. During prograde metamorphism of calc-silicate bearing rocks, the composition of fluid is affected by two factors, amount of infiltrating fluids and the buffering capacity of metamorphic reactions. Two end-member cases were considered by Labotka (1991); (1) fluid-dominated behavior and (2) rock dominated behavior. The former describes a situation where the buffering capacity of a rock is exceeded by the considerable amount of infiltrating fluids, while the latter describes system nearly closed or one in which the composition of fluids is internally buffered by metamorphic reactions. Since most of the prograde reactions in calcareous rocks produce CO_2-rich fluids, the amount of infiltrating fluids from external source can be constrained by the progress of decarbonation reactions. In this study, the effect of fluids during the evolution of mineral assemblages was surveyed and an estimation of fluid-rock ratio has been attempted on the basis of the modal abundance of progressively formed diopside in calc-silicate hornfels in the Hwanggangni formation of the Ogcheon belt, Korea which is composed of calcareous pebble bearing phyllite prior to contact metamorphism.

GEOLOGICAL SETTING

The study area consists of the Hwanggangni formation and the Cretaceous Daeyasan granite (Fig. 1). The Hwanggangni formation is composed of calcareous pebble bearing phyllite metamorphosed up to greenschist facies prior

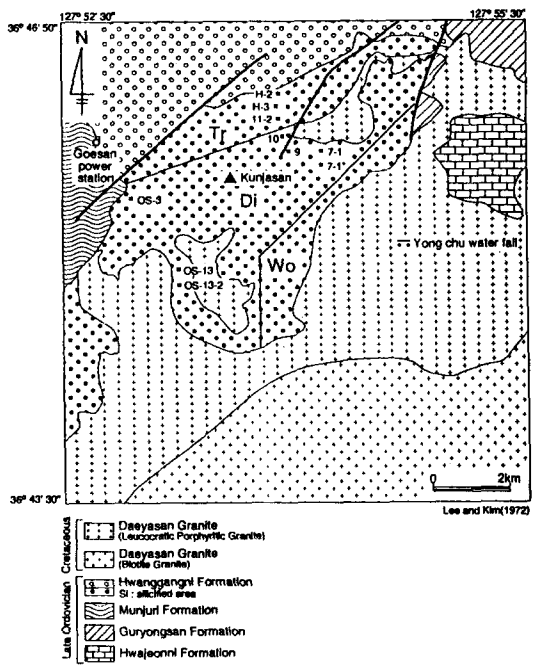

Fig. 1 Geological map including metamorphic zonation of the study area (modified from Lee and Kim, 1972). The squares stand for position of samples which are shown in Table 1 and Table 2. Tr, Di and Wo represent tremolite, diopside and wollastonite zone respectively.

to the contact metamorphism (Kim *et al.*, 1984). The Hwanggangni formation is dark gray in color and shows crenulation cleavages. The origin of the Hwanggangni formation has been interpreted as shallow marine environment sediments or glacial deposits (Lee and Kim, 1972). The size and kind of pebbles vary spatially and most of the pebbles are composed of crystalline limestone, quartzite, and granite. Some calcite and quartz pebbles are elongated along the foliation. The granite in the study area had been considered to be belonging to Sogrisan granite (Kim *et al.*, 1984 ; Hong, 1985) but recent isotope study on Cretaceous granite reveals that it is a different plutonic body, namely, Daeyasan granite (Jin *et al.*, 1993). The intrusion age of the Daeyasan granite is early Cretaceous (110 Ma by Rb/Sr whole rock dating) and the depth of intrusion is 1.5 ~ 5 Km or 0.5 ~ 1.3 Kbar in pressure (Jin *et al.*, 1993).

The calc-silicate hornfelses in the study area show bright color and contain tremolite-calcite-quartz-K-feldspar-phlogopite, diopside-grossular-vesuvianite and vesuvianite-diopside-wollastonite-phlogopite. Grossular and vesuvianite porphyroblasts are large enough to be identified in the field. Calcite and quartz in pebbles seem to have remained stable at all stages of contact metamorphism. Some calcite pebbles near intrusion contact, however, are rimmed by phlogopite. The first study of calc-silicate hornfels in the study area was made by Lee (1971). After his work, this hornfelsic lithology was named as Kunjasan formation by Kim and Yun (1980) who argued that this formation is related to the Hwanggangni formation by unconformity. In spite of successive studies, the field evidence of unconformity had been never reported and Kim *et al* (1984) and Hong (1985) concluded that this lithology is merely a contact metamorphosed Hwanggangni formation.

REPRESENTATIVE MINERAL CHEMISTRY

Table 1 contains analyses of diopside, tremolite, clinozoisite, and vesuvianite. The values of oxide sum in Table 1 refers to the conventional sum of metal oxide weight percents with all Fe as FeO except clinozoisite (Fe_2O_3). Location of samples are shown in Fig. 1. The composition of diopside is shown in Table 1 with Fe/Mg+Fe=0.01-0.2. The range of Fe/Fe+Mg of tremolite is 0.05-0.1. The composition of vesuvianite in 3 hornfelses are shown in Table 1. Composition of clinozoisite is shown in Table 1 with Al/Al+Fe=0.86-0.93. The Fe in clinozoisite is considered Fe^{+3} (Ferry, 1989).

MINERLOGICAL CHANGE DURING CONTACT METAMORPHISM

Mineralogical changes in calc-silicate rocks during contact metamorphism can be characterized by Bowen's decarbonation series in

Table 1. Mineral compositions of tremolite, diopside, vesuvianite and clinozoiseite detremined from electron microprobe analysis.

Sample	H-3	11-2	7-1	9	10	OS-13
	tremolite[1]	tremolite[1]	diopside[2]	diopside[2]	diopside[2]	diopside[2]
SiO_2	57.465	54.584	53.781	54.113	55.315	54.926
Al_2O_3	0.643	2.916	0.536	0.593	0.153	0.347
TiO_2	0.025	0.195	0.010	-	0.104	-
Cr_2O_3	-	-	-	-	-	-
FeO	2.076	4.507	5.164	6.518	0.402	1.928
MgO	22.506	19.626	14.263	13.793	18.009	17.095
MnO	0.023	0.432	0.147	0.176	0.097	
Na_2O	0.184	0.475	0.305	0.317	0.055	-
K_2O	-	0.088	0.266	-	-	-
CaO	13.663	13.265	24.886	25.272	26.23	26.190
Total	96.41	96.060	99.234	100.608	100.293	100.486
Si	7.95	7.71	1.978	1.990	1.987	1.99
Al	0.09	0.493	0.02	0.026	0.0086	0.013
Ti	0.002	0.017	0.0002	-	0.004	-
Cr	-	-	-	-	-	-
Fe^{+2}	0.24	0.535	0.159	0.199	0.013	0.058
Mg	4.64	4.139	0.782	0.756	0.966	0.924
Mn	0.0006	0.051	0.004	0.004	0.004	-
Na	0.006	0.119	0.01	0.022	0.004	-
K	-	0.015	0.006	-	-	-
Ca	2.03	2.00	0.981	0.9951	1.01	1.02

Sample	9	OS-13-2	7-1*	H-3	H-2	11-2
	vesuvianite[3]	vesuvianite[3]	vesuvianite[3]	clinozoisite[4]	clinozoisite[4]	clinozoisite[4]
SiO_2	36.160	35.709	35.915	38.266	37.489	37.825
Al_2O_3	15.960	15.974	15.960	28.464	26.891	29.179
TiO_2	1.241	3.003	1.241	0.119	0.104	-
Cr_2O_3	-	-	-	-	-	-
FeO	5.196	1.383	5.196	6.095	6.701	3.798
MgO	1.322	2.135	1.322	0.121	0.016	-
MnO	0.136	-	0.136	0.239	0.132	0.078
Na_2O	0.181	0.247	0.181	0.116	0.051	0.190
K_2O	0.011	-	0.011	-	-	-
CaO	35.702	37.147	35.702	24.296	23.987	24.074
Total	96.00	93.599	96.00	97.551	95.192	
Si	9.321	9.266	9.321	2.987	3.002	3.005
Al	4.870	4.867	4.870	2.617	2.54	2.728
Ti	0.232	0.593	0.232	0.005	0.005	-
Cr	-	-	-	-	-	-
Fe^{+2}	1.117	0.296	1.117	0.356	0.405	0.219
Mg	0.496	0.827	0.496	0.014	0.001	-
Mn	0.310	-	0.310	0.014	0.01	0.004
Na	0.093	0.124	0.093	0.019	0.008	0.028

1: cations per 23 oxygen atoms
2: cations per 6 oxygen atoms
3: cations per 38 oxygen atoms
4: cations per 12.5 oxygen atoms

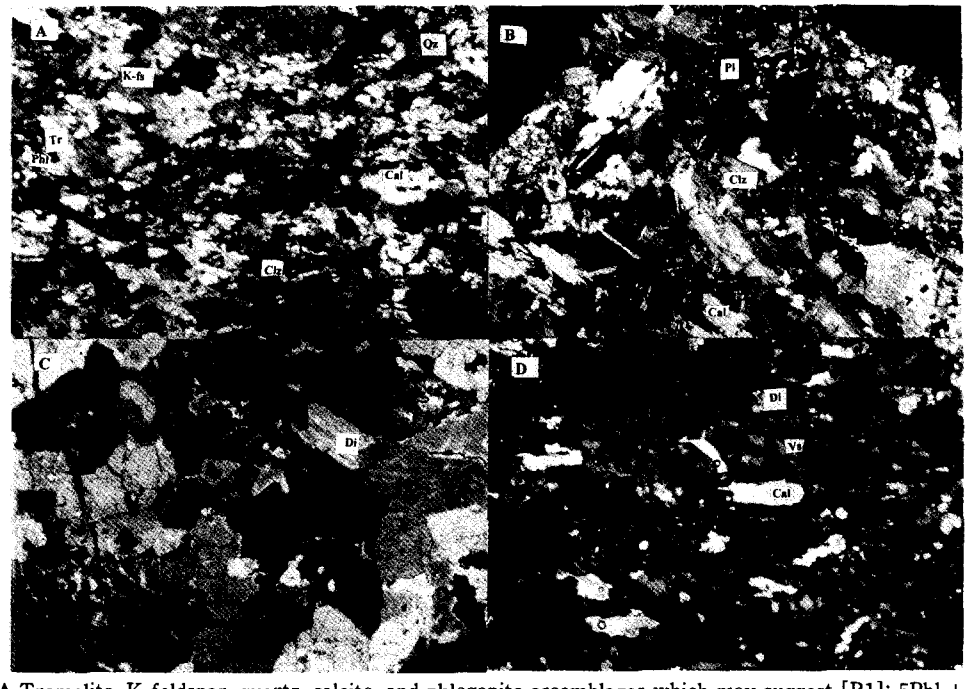

Fig. 2-A Tremolite, K-feldspar, quartz, calcite, and phlogopite assemblages which may suggest [R1]; $5Phl + 6Cal + 24Qz = 3Tr + 5Kfs + 6CO_2 + 2H_2O$.(X10, crossed polarized image.)
Fig. 2-B Calcite, plagioclase, and clinozoisite assemblages in tremolite zone which may suggest [R2]; $Cal + 3An + H_2O = 2Clz + CO_2$.(X10, crossed polarized image.)
Fig. 2-C Diopside. There are no reactant species with respect to [R3]; $3Cal + Tr + 2Qz = 5Di + H_2O + 3CO_2$.(X10, crossed polarized image.)
Fig. 2-D Calcite and diopside inclusions in vesuvianite porphyroblast. The reaction [R4]; $Silicate + Cal + H_2O = Vs + CO_2$ is inferred from these assemblages.(X10, crossed polarized image.)

which minerals involve in the order of talc, tremolite, diopside, forsterite, wollastonite, periclase, monticellite, ackermanite, tillieyite, spurite, rankinite, mervinite, and larnite as temperature increases (Bowen, 1940). This sequence is strictly valid in the system with the system components CaO-SiO_2-MgO, but may be used as general indicators for contact metamorphism in a more complicated system such as CaO-SiO_2-Al_2O_3-MgO-K_2O.

Mineralogical changes in this area can be characterized by three distinctive and diagnostic zones; the tremolite, the diopside, and the wollastonite zone (Fig. 1). This type of zonation is based on the appearance of minerals in accordance with Bowen's decarbonation series.

The matrix of pebble bearing phyllite mainly consists of calcite, quartz, K-feldspar, phlogopite, and plagioclase. Calcite in pebble bearing phyllite occurs as matrix forming mineral, pebbles and veins. Quartz is also major component of matrix and pebbles. Most of pebbles are composed of calcite and quartz. Some calcite and quartz which comprise pebbles exist near innermost part of the aureole and have not been affected by prograde metamorphic reactions.

The mineral which first overprints regional metamorphic and deformation texture such as crenulation cleavages is tremolite. Tremolite occurs across the cleavages as radial aggregation or columnar individual crystals. In the tremolite zone, coexisting minerals are mica, plagioclase, K-feldspar, calcite, quartz, and clinozoisite. One of the probable reactions

of tremolite formation on the basis of the observed assemblages (Fig. 2-A) is (Berman, 1988);

$$5Phl + 6Cal + 24Qz = 3Tr + 5Kfs + 6CO_2 + 2H_2O \quad [R1]$$

Clinozoisite is columnar and the formation of clinozoisite may also be deduced from the assemblages (Rice and Ferry, 1982, Fig. 2-B);

$$Cal + 3An + H_2O = 2Clz + CO_2 \quad [R2]$$

Calc-silicate hornfelses in diopside zone mainly contain diopside, grossular, and vesuvianite. In the diopside zone, typical mosaic hornfelsic textures are observed. Diopside crystals are the most abundant phases showing polygonal crystal shape, and this trend becomes weaker away from the intrusion contact. Vesuvianite occurs as subhedral porphyroblast (up to 1.5 cm) with numerous calcite, diopside, and sometimes clinozoisite inclusions. Grossular also occurs as porphyroblast with diopside, calcite, and vesuvianite inclusions. These inclusions may suggest the probable reactions. Matrix of hornfels in this zone is mainly composed of diopside (modal percent up to 94 %) and there is no considerable amount of reactant species except remnants of pebbles mainly consist of quartz and calcite. A probable reaction of diopside formation is (Berman, 1988, Fig. 2-C);

$$3Cal + Tr + 2Qz = 5Di + H_2O + 3CO_2 \quad [R3]$$

Formation of vesuvianite is deduced from inclusions (Fig. 2-D). Vesuvianite might be formed by the reaction (Valley *et al.*, 1985);

$$Silicate + Cal + H_2O = Vs + CO_2 \quad [R4]$$

In the study area, possible silicate minerals in the reaction [R4] are diopside or clinozoisite since they occur as inclusions in vesuvianite. Some vesuvianite porphyroblasts show oscillatory zoning. Yardley and Loyd (1995) suggested that this type of zoning is strong evidence for infiltration of external fluid because external disturbance may form zonation patterns. In spite of textural evidence that indicates vesuvianite was involved in grossular formation (i.e., inclusion relation), it is difficult to pinpoint a single reaction of grossular formation because there are several possible reactions involving vesuvianite yielding grossular.

Assemblages in the wollastonite zone are very similar to those of the diopside zone except wollastonite and phlogopite. Individual crystals of wollastonite are bladed shape. The reaction of wollastonite formation is difficult to constrain because of the lack of textural evidence for possible reactions. Phlogopite is always associated with calcite and some calcite pebbles are rimmed by phlogopite. Hence one of the probable reaction of phlogopite formation is (Rice, 1977);

$$6Cal + Kfs + 3Tr = Phl + 12Di + 2H_2O + 6CO_2 \quad [R5]$$

FLUID-ROCK RATIO, FLUX AND PERMEABILITY

Modal analysis of diopside had been carried out for 12 thin sections, and phlogopite-free samples were used to estimate the fluid-rock ratios (Table 2). Phlogopite-free samples were chosen in order to estimate the fluid-rock ratios based on the lower temperature reaction [R3] in which phlogopite is absent and diopside occurs as product phase.

Table 2. Modal abundance data of samples used for calculating fluid-rock ratio. OS-3, 7-1, and 7-1* are samples in diopside zone which contain no phlogopite. Vesuvianite porphyroblasts are most abundant in 7-1*

	OS-3	7-1*	7-1
diopside	82.9	70.2	94.5
vesuvianite	12.5	29.8	
grossular	1.2		
others	3.4		5.5

The modal abundance of diopside in each sample was converted to progression variable defined below. Amount of infiltrating fluid is given by the equation, (Ferry, 1986; Spear, 1993)

$$n^a_{fOT} = -\xi \times \frac{(X^f_{CO_2} v_{H_2O} - X^f_{H_2O} v_{CO_2})}{X^f_{CO_2} - X^a_{CO_2}} \quad (1)$$

ξ : progressive variable=(moles of product)/(coefficient of product)

$X^f_{CO_2}$: final fraction of CO_2

$X^f_{H_2O}$: final fraction of H_2O

v_{H_2O} : stoichiometric coefficient of H_2O

$X^a_{CO_2}$: initial fraction of CO_2

v_{CO_2} : stoichiometric coefficient of CO_2

n^a_{fOT} : moles of infiltrating fluid

The equation (1) is based on the fact that metamorphic reactions in the calcareous rocks produce CO_2-rich fluids and consequently the reaction progress can monitor amount of volumes of hydrous fluids infiltrated from external source. The reaction [R3] was selected in this study. Thus, in this case product mineral is diopside and progressive variable can be calculated by modal percent of diopside. For example, consider a rock contains α % of diopside. If the molar volume of diopside is β cm^3/mole, then 100 cm^3 rock has α cm^3=α/β moles of diopside. Since the stoichiometric coefficient of diopside is 5 in [R3], the progressive variable ξ=$\alpha/\beta \div 5$ in this case.

The initial composition of infiltrating fluids is assumed to be pure H_2O. Consequently, the calculation will yield a minimum estimation of infiltrating fluids. In order to find plausible $X^f_{co_2}$ values of final state, phase equilibria in T-X_{co_2} space and mineral assemblages must be considered. The T-X_{co_2} diagrams in this study were drawn by TWEEQU (Berman, 1991) with system components Al_2O_3-CaO-MgO-SiO_2-K_2O-H_2O-CO_2. All calorimetric data of solid phases was taken from Berman (1988) for the sake of internal consistency and those of volatile phases from Helgason and Kirkham (1974) were used for the same reason. Reac-

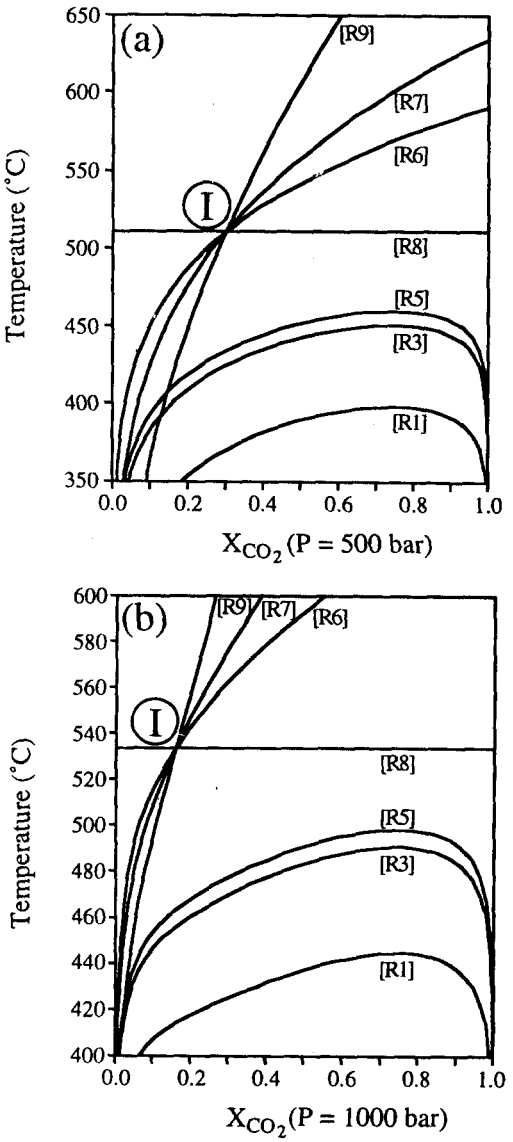

Fig. 3 Inferred reactions in the T-X_{co_2} diagrams (by TWEEQU, Berman, 1991). (a) At 0.5 Kbar. (b) At 1 Kbar. [R1]: 5Phl + 6Cal + 24Qz = 3Tr + 5Kfs + $6CO_2$ + $2H_2O$, [R3]: 3Cal + Tr + 2Qz = 5Di + H_2O + $3CO_2$, [R5]: 6Cal + Kfs + 3Tr = Phl + 12Di + $2H_2O$ + $6CO_2$, [R6]: Cal + Qz = Wo + CO_2, [R7]: An + Cal + Qz = Gr + CO_2, [R8]: Gr + Qz = An + Wo, [R9]: An + Wo + Cal = Gr + CO_2.

tions in T-X_{co_2} diagrams are shown in Fig. 3 (a) and (b) for the conditions of 0.5 and 1 Kbar since these values correspond to the range of the inferred intrusion depth of Daeyasan granite (Jin *et al.*, 1993). Ideal mixing of volatile phases is assumed and pure end-member composition is assumed for solid phases. The small change in relative position of reaction curves in T-X_{co_2} diagrams due to the variation of mineral composition in the study area cause no significant error in fluid-rock ratio calculation because small change in temperature can not cause large deviation of molar volume of fluids. In these diagrams, every reaction curve for the formation of tremolite, diopside and phlogopite shows steep slope in hydrous portion and this region is bounded by X_{co_2} value corresponding to the invariant point I (Fig. 3) made by following reactions;

$$Cal + Qz = Wo + CO_2 \quad [R6]$$
$$An + 2Cal + Qz = Gr + CO_2 \quad [R7]$$
$$Gr + Qz = An + 2Wo \quad [R8]$$
$$An + Wo + Cal = Gr + CO_2 \quad [R9]$$

There are two cases in the choice of probable $X^f_{CO_2}$ by following criteria.

Case 1. $X_{co_2} \leq 0.2$

In the diopside zone, diopside coexists with vesuvianite and upper limiting value of its stability field is less than X_{co_2} value of the invariant point I in Fig. 3 (Valley *et al.*, 1985; Hochella *et al.*, 1982; Labotka *et al.*,1988). Valley *et al.* (1985), calculated upper limiting value for vesuvianite on the basis of former experiment (Hochella *et al.*,1982), argued that at $P \leq 2$ Kbar, the position of invariant point I is near $X_{co_2} = 0.2$. However, in Fig. 3, this position is located above 0.2 at 0.5Kbar and below this value at 1Kbar. This is due to the discrepancy between calorimetric data used in their calculation and database in the TWEEQU. This value will be taken as one of the probable $X^f_{CO_2}$ in this study.

Case 2. $X_{co_2} \leq 0.02$

This value can be used as a probable upper limiting value in diopside zone if the following two conditions are satisfied.

1. $X_{CO_2,tr} \geq X_{CO_2,di}$ $X_{CO_2,wo}$ and
2. $X_{CO_2,tr} \leq 0.02$.

Where $X_{CO_2,tr}$, $X_{CO_2,di}$ and $X_{CO_2,wo}$ represent X_{CO_2} in the tremolite, diopside, and wollastonite zone, respectively. The first condition represents a situation in which the composition of fluids had been more hydrous toward the intrusion contact. In the tremolite zone, there are T-X_{co_2} univariant assemblage with respect to reaction [R1], whereas in the diopside zone, there are no significant amount of reactant species of reaction [R3], suggesting nearly complete reaction [R3] during contact metamorphism. This may suggest lower X_{co_2} in the diopside zone. Hong (1985) also reported gradual increment of andradite fraction in grossular in the study area toward the intrusion and this trend implies that the composition of metamorphic fluids had become more hydrous toward intrusion contact (Taylor and O'Neil, 1977; Labotka *et al.*, 1988). These two consideration suggest the likelihood of the first condition. As mentioned in the previous section, clinozoisite was formed by [R2] in the tremolite zone. This reaction is strongly exothermic and can not be driven from left to right at a condition of increasing temperature during contact metamorphism. The reaction, however, is known to proceed when the fluid composition is H_2O-rich (Rice and Ferry, 1982). Tracy and Frost (1991) pointed out the upper limiting value of X_{co_2} for clinozoisite stability field is 0.02 at 1Kbar. Thus X_{co_2} in tremolite zone was probably less than 0.02. Then condition 1 and 2 might have been satisfied during metamorphism and consequently $X_{co_2} = 0.02$ is probable upper limiting value in diopside zone.

Table 3. Fluid-rock ratios calculated by the equation(1)

	OS-3				7-1*				7-1			
P (Kbar)	0.5 (Kbar)	0.5 (Kbar)	1.0 (Kbar)	1.0 (Kbar)	0.5 (Kbar)	0.5 (Kbar)	1.0 (Kbar)	1.0 (Kbar)	0.5 (Kbar)	0.5 (Kbar)	1.0 (Kbar)	1.0 (Kbar)
V_{H_2O}	23.166	23.166	44.789	25.940	23.166	23.166	44.789	25.940	23.166	23.166	44.789	25.940
X_{CO_2}	0.2	0.02	0.2	0.02	0.2	0.02	0.2	0.02	0.2	0.02	0.2	0.02
X_{H_2O}	0.8	0.98	0.8	0.98	0.8	0.98	0.8	0.98	0.8	0.98	0.8	0.98
ξ	0.25	0.25	0.25	0.25	0.21	0.21	0.21	0.21	0.28	0.28	0.28	0.28
n	2.75	36.5	2.75	36.5	2.31	30.66	2.31	30.66	3.08	40.88	3.08	40.88
F/R	0.64	8.4	1.2	9.4	0.53	7.1	1.03	7.9	0.72	9.5	1.4	10.6

Table 4. T.I.F calculated by the equation (2) (Unit: cm^3/cm^2)

	OS-3		7-1*		7-1	
P(KBar)	0.5(KBar)	1(KBar)	0.5(KBar)	1(KBar)	0.5(KBar)	1(KBar)
1(KBar)	1.2×10^{4} r cm^3/cm^2	2.2×10^{4} r cm^3/cm^2	3.9×10^{3} r cm^3/cm^2	7.6×10^{3} r cm^3/cm^2	5.3×10^{3} r cm^3/cm^2	1×10^{4} r cm^3/cm^2
X_{CO_2}=0.2	4.5×10^{4} c cm^3/cm^2	8.4×10^{4} c cm^3/cm^2	1.5×10^{4} c cm^3/cm^2	2.9×10^{4} c cm^3/cm^2	2×10^{4} c cm^3/cm^2	8.4×10^{4} c cm^3/cm^2
X_{CO_2}= 0.02	6.1×10^{4} r cm^3/cm^2	1.7×10^{5} r cm^3/cm^2	7×10^{4} r cm^3/cm^2	1.4×10^{5} r cm^3/cm^2	5.24×10^{4} r cm^3/cm^2	1.4×10^{4} r cm^3/cm^2
X_{CO_2}= 0.02	5.8×10^{5} c cm^3/cm^2	6.58×10^{5} c cm^3/cm^2	2.0×10^{5} c cm^3/cm^2	2.2×10^{5} c cm^3/cm^2	2.7×10^{5} c cm^3/cm^2	3.0×10^{5} c cm^3/cm^2

r: based on the assumption of vertical intrusive contact.
c: based on the assumption of gently dipping intrusive geometry.

Time Integrated Flux and Permeability

The calculated fluid-rock ratios by equation (1) are shown in Table 3. The calculation of flux can be made under the assumption of volumes of fluids which are equivalent to fluid-rock ratio had passed through a unit volume of rocks during metamorphism. Simple way to calculate time integrated flux (T.I.F) is (Ferry, 1989);

$$\text{Fluid- rock ratio} \times 1\text{cm} \times 1\text{cm} \times \text{Lcm}/\text{cm}^2 = \text{T.I.F}\ (\text{cm}^3/\text{cm}^2) \quad (2)$$

Where L is the thickness of rocks which record same fluid-rock ratio. Two cases for the calculation of T.I.F are considered in this study; the intrusion contact to the diopside zone distance (1) assuming a vertical intrusive contact. (2) assuming a intrusive contact dipping 15°. The second assumption was based on the postulation of Hong(1985) who observed intermittent exposures of granite outcrops along Ssanggok valley and argued that a gently dipping intrusion geometry in the study area. The calculated T.I.F by equation (2) are shown in Table 4 and range from 10^4 to 10^6 cm^3/cm^2. Since the calculated fluxes are time integrated, in order to yield permeabilities, total duration of metamorphic event must be known under the assumption of Darcian flow. If the Daeyasan pluton has a slab geometry with its half width 3 Km, then time for thermal decay is given by (Carslaw and Jaeger, 1959, 60-73; Spear, 1993, 43-45);

$$t = h^2/k = (3\times10^3)^2\ m^2/10^{-6}\ m^2/\text{second} = 9\times10^{12}\ \text{second} \quad (3)$$

h: half width of a slab
k: thermal diffusivity (taken from average rock property)

From equation (3), the total duration is 2.8×10^5 years. The cooling by conduction and simple geometry of pluton are assumed in calculation of time for thermal decay by equation (3). There are, however, additional factors which affect time for thermal decay; (1) exact geometry of pluton. (2) latent heat of fusion of magma. (3) possibility of convection. (4) erosion or burial that may be occurring as the pluton cools. Numerical modeling considering these factors have been done (Norton and Knight, 1977; Harrison and Clarke, 1979). According to these models, the order of time for thermal decay is 10^5~10^6 year and that is approximately same time constant obtained from the equation (3). Hence usage of the equation (3) may give reasonable approximation of time for cooling. The calculated time, however, is maximum estimation because duration of prograde metamorphic reactions is shorter than time for thermal decay. In spite of this uncertainty, error in range of the calculated flux is not great because change in the exponent of 10 in time of flow is not considerable. This will be discussed in the next section. Convection is only important when aureole is considerably cooled. Brittle fracturing is avaliable at this stage. The fracturing enhance permeability and touch off flow of meteoric fluids. This process involves retrograde reactions and is not significant in prograde metamorphism. The pressure gradient that produced by thermal buoyancy is on the order of 0.015×10^5 Pa/m, and viscosity of fluids in this case is 10^{-4} Pa second (Walther and Orville, 1982; Walther and Wood, 1984). Thus permeability (k) can be calculated by Darcy's law (Spear, 1993);

$$K = Qv\,\eta/(dp/dz) \div \text{duration of event} \quad (4)$$

η: viscosity
Qv: T.I.F
dp/dz: pressure gradient along flow

The petrological meanings of calculated permeabilities in this manner will be discussed in the next section.

DISCUSSION

Validity of Assumptions in This Study

Two major assumptions which have been used in this study are; (1). The assumption of equivalent volumes of fluids corresponding to fluid-rock ratio had been passed through rock body. (2). The observed reaction progress is solely due to the competition between buffering process and infiltration of external fluids. The first assumption had been made in previous studies on fluid-rock interactions (Ferry, 1989). Labotka (1988), however, in his study on Notch peak aureole, pointed out that the volumes of fluids corresponding to fluid-rock ratio does not necessarily indicate volumes of fluids which had been passed through rock body. In the wollastonite zone of Notch peak aureole, the fluid-rock ratio is up to 13, but in the adjacent isograde (diopside zone), fluid-rock ratio is below 0. 1. Labotka (1988) argued that if volumes of fluids represented by fluid-rock ratio in wollastonite zone is interpreted as volumes of fluids which had been flowed through rock body during metamorphism, there are no explanation for low fluid-rock ratio (less than 0.1) in diopside zone of Notch peak aureole. Thus Labotka (1988) concluded that the recorded fluid-rock ratio in wollastonite zone of Notch peak aureole does not indicate volumes of fluids which had been passed through rock body but indicate volumes of static reservoir which contain fluids that had been interacted with rocks in wollastonite zone. In the study area, however, fluid-rock ratios in diopside zone generally more than 1 and also assemblages in tremolite zone indicate both buffering and maintenance of H_2O-rich fluids during metamorphism. Since buffering process alone may produce CO_2-rich fluids in the calcareous rocks, assemblages in the tremolite zone imply that infiltration of external

fluids accompanied by buffering. Consequently, both high fluid-rock ratio in diopside zone and mineral assemblages in tremolite zone may reflect the prevalence of infiltration of external fluids during contact metamorphism in the study area and this may support the first assumption in this study.

The Rayleigh distillation by which the reaction products do not mix to produce homogeneous fluids but are selectively removed (distilled) from rock and this process could also produces significant reaction progress because the fluids remaining in the rock would be out of equilibrium, thus promoting further reaction. This can be triggered by addition of other solute, like NaCl, which greatly reduces the activity of H_2O and expands the region of immiscibility. Even if distillation had been occurred during metamorphism, it does not, however, necessarily indicate progress of reaction without infiltration in the study area because of following two reasons. In the tremolite zone where strongly exothermic reaction [R2] yielded clinozoisite, only possible when massive infiltration of H_2O-rich fluids overcome the exothermic effect. Additionally, the formation of OH-bearing species such as vesuvianite and clinozoisite requires amount of H_2O, thus could not be formed by CO_2 removal alone by Rayleigh distillation. Therefore the second assumption may be hold approximately even if distillation had been occurred during contact metamorphism.

Reaction Progress and Metamorphic Zonation

The calculation of fluid-rock ratio in this study was based on measured reaction progress of [R3]. The implicit assumption in calculation of fluid-rock ratio is that observed modal abundance of diopside was solely due to the reaction progress of [R3]. Hence if diopside in samples which used in calculation of fluid-rock ratio was produced by any other reactions than [R3], the calculated fluid-rock ratio may be uncertain. In the study area, however, as mentioned in the previous section, occurrence of mineral assemblage indicating H_2O-rich component of metamorphic fluids may suggest that at least the qualitative feature of metamorphism drawn by this study is plausible.

The name of metamorphic zonation in the study area is according to index minerals which are shown in Bowen's decarbonation series. In fluid dominated system, however, the name 'wollastonite zone' may not have absolute meaning because wollastonite can be formed near 400℃ in H_2O-rich environment and consequently it can not indicate significantly higher temperature than that of diop-

Table 5. Permeabilities calculated by the equation (4) Unit: (m^2)

	OS-3		7-1*		7-1	
P(KBar)	0.5(KBar)	1(KBar)	0.5(KBar)	1(KBar)	0.5(KBar)	1(KBar)
X_{CO_2}=0.2	r 7.2×10^{-19} m^2	r 1.3×10^{-18} m^2	r 2.3×10^{-19} m^2	r 4.6×10^{-18} m^2	r 3.2×10^{-19} m^2	r 6×10^{-19} m^2
X_{CO_2}=0.2	c 2.7×10^{-18} m^2	c 5.0×10^{-18} m^2	c 9×10^{-18} m^2	c 1.7×10^{-18} m^2	c 1.2×10^{-18} m^2	c 2.4×10^{-18} m^2
X_{CO_2}=0.02	r 3.7×10^{-18} m^2	r 1×10^{-17} m^2	r 4.2×10^{-18} m^2	r 8.4×10^{-18} m^2	r 3×10^{-18} m^2	r 1.1×10^{-17} m^2
X_{CO_2}=0.02	c 3.5×10^{-17} m^2	c 4×10^{-17} m^2	c 1.4×10^{-17} m^2	c 1.4×10^{-17} m^2	c 1.6×10^{-17} m^2	c 1.8×10^{-17} m^2

r: based on the assumption of vertical intrusive contact.
c: based on the assumption of gently dipping intrusive geometry.

side stability field in this case.

Petrological Implication of Overall Results

From Table 3, it is clear that, in any case, the fluid-rock ratios are more than 0.5 and generally much more than 1. This indicate volumes of metamorphic fluids which had been interacted with rocks during contact metamorphism are larger than those of rocks. Table 5 shows the resulting permeabilities (from equation (4)). In spite of geometrical consideration discussed in the previous section, resulting permeabilities are nearly identical in both cases (on the order of $10^{-19} \sim 10^{-17}$ m^2). These estimated values in the study area are not atypical in the contact aureoles and belong to measured permeability range of unfractured crystalline rocks (10^{-22}~10^{-16} m^2, Hanson, 1995). The fact that the calculated permeability is lower than that of fractured rock (more than 10^{-15} m^2) is a reasonable consequence because channelized flow along macroscopic fracture generally occurred during cooling stage but not in the peak metamorphic event (Hanson, 1995; Norton and Knight, 1977; Furlong *et al.*, 1991). In natural rocks, this behavior of metamorphic fluid can be detected by isotope monitor (Cliffored and Evans, 1993). Estimated permeabilities by Baumgartner and Ferry (1991), Ferry (1989), and Ferry and Dipple (1991) are on the order of $1 \sim 100 \times 10^{-18}$ m^2 during peak metamorphism in serveral system on the basis of reaction-transport model and observed reaction phogress in calc-silicate rocks.

The time calculated by equation (3) might yield maximum value because time interval for prograde reaction is fraction of time for thermal decay. Hence attempt has been made to calculate length of time interval of corresponding temperature range in which the reaction [R3] can be activated. These temperature intervals are 400~460℃ at 1 Kbar and 350~430℃ at 0.5 Kbar. Calculation have been done under the assumption of slab intrusion geometry and country rock temperature 200℃ which is lower limiting temperature of greenschist facies. The temperature of intrusion is assumed to be 700℃. Resulting length of time interval is 1.2~7.6 x 10^{12} second. This value is shorter than that calculated by equation (3) but it is on the order of 10^{12} second. Permeability may slightly enhanced by these values, however, this permeability still belong to range of unfractured crystalline rocks.

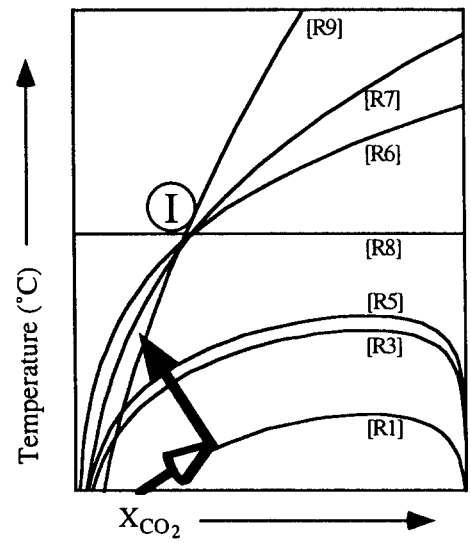

Fig. 4 Inferred reaction pathways. Arrow shows possible course of the compositional change of metamorphic fluids.

In tremolite zone, the observed assemblages contain both reactant and product phases with respect to reaction of tremolite formation [R1], whereas in diopside zone, there are no considerable amount of reactant phases with respect to [R3]. Hence, in spite of evidence for H_2O-rich environment (occurrence of clinozoisite), it seems the composition of metamorphic fluids in tremolite zone had been effectively buffered by [R1] during metamorphism. The complete reaction of [R3] in diopside zone indicate buffering capacity of rocks had been exceeded by massive infiltration of external fluids. The reaction pathway inferred from these two different trends of fluid-rock interactions are qualitatively shown in Fig. 4.

In Fig. 4, the arrow along reaction curve of [R1] indicate composition of metamorphic fluids are buffered by [R1] and the other arrrow nearly normal to the arrow along [R1] indicate composition of metamorphic fluids become more hydrous by infiltration of external fluids and loss of buffering capacity of rocks in diopside zone. According to the terminology proposed by Labotka (1991), the mineral assemblages in tremolite zone and diopside zone show 'rock-dominated behavior' and 'fluid-dominated behavior' during contact metamorphism. In tremolite zone, however, there are indicators of both H_2O-rich environment and buffering process. Thus the way of fluid-rock interaction in the tremolite zone is more properly termed as combination of infiltration and buffering (Rice and Ferry, 1982).

The fluid dominated behavior has been documented primarily aureoles containing argillaceous limestone or calcareous argillite (so called 'metamorphic aquifer' Labotka, 1991; Dunn, 1995; Heinrich, 1994; Cartwright and Oliver, 1994; Labotka *et al.*, 1988), whereas most of rock dominated behavior (buffered system) has been reported for progressive metamorphism of marbles and siliceous dolomite (so called 'metamorphic aquitard' Labotka, 1991; Rice, 1977). So the prevalence of infiltration of external fluids may be owing to the lithology of the study area.

CONCLUSION

(1) Two different trends of fluid-rock interactions are recognized in the study area; The combination of infiltration and buffering in tremolite zone and fluid dominated behavior in diopside zone.

(2) Calculated range of fluid-rock ratio and permeability is 0.6~9 and 10^{-19}~10^{-17} m^2 respectively. Range of permeability constrained in this study shows good agreement with already documented data in previous works in other contact metamorphic aureoles and within the range of unfractured crystalline rocks.

ACKNOWLEDGEMENT

We are grateful to Dr. Y.D. Park in Korea University, Prof. S. T. Kwon in Yonsei University, Prof. C.W. Oh in Chonbuk University and Prof. M. Cho in Seoul National University for their constructive reviews and discussions.

This work was partially suppoted by 1996 fund of KOSEF.

REFERENCES

Baumgartner, L.P., and Ferry J.M., 1991, A model for coupled fluid-flow and mixed-volatile mineral reactions with applications to regional metamorphism. Contrib. Mineral. Petrol., 106, 273-285.

Berman, R.G., 1988, Internally consistent thermodynamic data for minerals in the system Na_2O - K_2O - CaO - MgO - FeO - Fe_2O_3 - Al_2O_3 - SiO_2 - TiO_2 - H_2O - CO_2. J. Petrol., 29, 445-522.

Berman, R.G., 1991. TWEEQ (version 1.0) Thermobarometry with estimation of equilibration state.

Bowen, N.L., 1940. Progressive metamorphism of silicious limestone and dolomite. J. Geol., 48, 225-274.

Carslaw, H.S., and Jaeger, J.C., 1959, Conduction of heat in solid. Clarendon Press, Oxford., 510p.

Cartwright, I., and Oliver, H.S.N., 1994, Fluid flow during contact metamorphism at Mary Kathleen, Queensland, Australia. J. Petrol., 35, 1493-1519.

Clifford, S.T., and Evans. B.W., 1993, Limited fluid-rock interaction at marble-gneiss contacts during Cretaceous granulite-facies metamorphism, Seward Penisula, Alaska. Contrib. Mineral. Petrol., 114, 27-41.

Dunn, S.R., 1995, Mineral equilibria in amphibolite facies marble, S. Ontario and duplications for T-X_{co_2} relations. Abst. Program., Geol. Soc. Am.

Ferry, J.M., and Dipple G.M., 1992, Models for coupled fluid flow, mineral reaction, and isotopic alteration during contact metamorphism: The Notch peak aureole, Utah. Am. Mineral., 77, 577-591

Ferry, J.M., 1989, Contact metamorphism of roof pendant at Hope Valley, Alpine County, California, U.S.A. Contrib. Mineral. Petrol., 101, 402-417.

Furlong, K.P., Hanson, R.B., and Bowers, J.R., 1991, Modeling thermal regimes. In Contact metamorphism, Rev. Mineral., 26(eds. Kerrick, D.M.)

mineral. Soc. Am., 437-503.

Hanson, R.B., 1995, The hydrodynamics of contact metamorphism. Geol. Soc. Am. Bull., 107, 595-611.

Harrison, T.M., and Clarke, G.K.C., 1979, Model of the thermal effect of igneous intrusion and uplift as applied to Quottoon pluton, British Columbia. Can. J. Earth. Sci., 16, 411-420.

Heinrich, W., and Gottschalk, M., 1994, Fluid flow patterns and infiltration isograds in melilite marbles from the Bufa del Diente contact metamorphic aureole, north east Mexico. J. Metamorphic. Geol., 12, 345-359.

Helgason, H.C., and Kirkham, D.H., 1974, Theoritical prediction of the thermodynamic behavior of aqueous electrolytes at high pressures and temperatures. I. Summary of the thermodynamic/electrostatic properties of the solvent. Am. J. Sci., 274, 1089-1198.

Hochella, M.F., Liou, J.G., Keskinen M.J. and Kim, H.S., 1982, Synthesis and stability relation of magnesium idocrase. Economic. Geol., 77, 798-808.

Hong, S.S., 1985, A petrographic study on the contact metamorphism of the Ogcheon formation with Sogrisan granite in the southeastern Goesan area. MS thesis, Yonsei Univ., 76p.

Jin, M.S., Kim, S.J., Chi, S.J., Shin S.C., and Choo, S. H., 1993, Radiometric ages of the Paleozoic and Mesozoic Granites in the middle part of the Ogcheon fold belt. KIGAM, Research Report., 34p.

Kim, H.S., Kim, Y.K., and Lee, J.R., 1984, Polymetamorphism of the Ogcheon metamorphic belt in the Hwayang-ri District, Goesan-gun, Chungbuk Province. Collection of papers in Science and Engineering., 25, Korea. Univ., 203-218.

Kim, O.J, and Yun, J.S., 1980, Petrological study and tectonic interpretation of the upper Ogcheon group. Mining. Geol., 13, 91-103.

Labotka, T.C., Nabelec, P.I., and Papike, J.J., 1988, Fluid infiltration through the Big-Horse limestone member in the Notch Peak Contact-metamorphic aureole, Utah. Am. Mineral., 73, 1302-1324.

Labotka, T.C., 1991, Chemical and physical properties of fluids. In Contact metamorphism, Rev. Mineral., 26(eds. Kerrick, D.M.), Mineral. Soc. Am., 43-104.

Lee, C.H. and Kim, J.H., 1972, Explanatory text of the geological map of Goesan sheet. Geological Survey of Korea, 22p.

Lee, D.S., 1971, Study on the igneous activity in the middle Ogcheon geosynclinal zone. J. Geol. Soc. Korea., 7, 153-216.

Norton, D., and Knight, J., 1977, Transport phenomena in hydrothermal system: cooling of plutons. Am. J. Sci., 277, 937-981.

Rice, J.M., 1977, Progressive metamorphism of impure dolomitic limestone in the Marysville aureole, Montana. Am. J. Sci., 277, 1-24.

Rice, J.M., and Ferry, J.M., 1982, Buffering, infiltration and the control of intensive variables during metamorphism. In Characterization of metamorphism through mineral phase eqilibria, Rev. Mineral., 10(eds. Ferry, F.M.), Mineral. Soc. Am., 263-326.

Spear, F., 1993, Metamorphic phase equilibria and pressure-temperature-time paths. Book Crafters, Inc., Chelsea, Michigan, 799p.

Taylor, B.E., and O'Neil,R., 1977, Stable isotope studies of metasomatic Ca-Fe-Al-Si skarns and associated metamorphic and igneous rocks, Osgood Mountain, Nevada. Contrib. Mineral. Petrol., 63, 1-49.

Tracy, R.J., and Frost B.R., 1991, Phase equilibria and thermobarometry of calcareous, ultramafic, mafic rocks, and iron formation. In contact metamorphism, Rev. Mineral., 26, (eds. Kerrick, D.M.), Mineral. Soc. Am. 207-289.

Valley, J.W., Peacor, D.R., Bowman, J.R., Essen, E. J., and Allard, M.J., 1985, Crystal chemistry of a Mg-vesuvianite and implication for phase equilibria in the system CaO-MgO-Al_2O_3-SiO_2-H_2O-CO_2. J. Metamorphic. Geol., 3, 137-153.

Walther, J.V., and Orville, P.M., 1982, Volatile production and transport in regional metamorphism. Contrib. Mineral. Petrol., 79, 252-257

Walther, J.V., and Wood, B.J., 1984. Rate and mechanism in prograde metamorphism. Contrib. Mineral. Petrol., 88, 246-259.

Yardley, B.D.W., and Loyd, G.E., 1995, Why metasomatic fronts are really metasomatic sides. Geology, 23, 53-56.

(책임편집 : 권성택)

괴산지역 황강리층의 접촉변성작용에서 유체-암석 간의 상호작용에 관한 연구

김상명 · 김형식

서울특별시 성북구 안암동 5-1(136-107), 고려대학교 이과대학 지구환경과학과

요 약 : 괴산지역 중생대 백악기 대야산화강암체 근방의 황강리층 석회규산염 혼펠스는 투각섬석-클리노조이사이트-알칼리장석-방해석, 투휘석-그로슐라-베수비아나이트, 규회석-투휘석-그로슐라-베수비아나이트 등의 변성광물군으로 특징지워지며, 이들 광물군은 접촉변성시 낮은 X_{CO_2}조건을 지시해준다. 본 연구지역에서 두가지 유형의 접촉변성작용시의 유체-암석 간의 상호작용이 인지되었다. 하나는 접촉변성대 외각에서의 투과작용과 완충작용의 조합이고, 다른 하나는 대부분의 접촉변성대에서 인지되는 외부유체의 대량투과이다. 본 연구에서는 접촉변성시의 유체/암석비와 이 비에 해당하는 부피의 유체가 암석을 통해 이동하였다는 가정하에서 투수도를 계산하기 위하여 투휘석의 모달 퍼센트를 측정하였다. 이와같은 방법으로 계산된 유체/암석비는 0.6~9이고 투수도는 10^{-19}~$10^{-17}m^2$이다. 이 값들은 다른 지역의 석회질산규산염암 접촉변성대들에서 구하여진 수치들과 좋은 일치를 보여주며, 이론적 연구에 의해 전진적 변성작용시에 예상되어지는 수치이다.

핵심어 : 유체-암석 상호작용, 유체-암석비, 투수도, 석회규산염 혼펠스